Predicting Fluid-Bed Reactor Efficiency Using Adsorbing Gas Tracers

Gas tracers have been used frequently to predict conversion in chemical reactors. But in heterogeneous systems such as fluid-bed reactors, tracer residence time data usually overpredict actual contact time and conversion. In this work, the general two-phase countercurrent flow model is extended to include tracer adsorption, which is important in predicting contact time. The tracer used was SF_6, whose adsorption on the solids could be varied over a wide range. The apparent reactor efficiency, calculated directly from tracer response, is shown to approach that estimated from the two-phase model when the fluid bed approached homogeneity. This is the case for many large-scale reactors that are operated in the turbulent fluidization regime. The use of horizontal baffles in methanol-to-gasoline cold flow models is shown to improve bed efficiency by staging the bed.

F. J. Krambeck, A. A. Avidan, C. K. Lee, M. N. Lo
Mobil Research and Development Corporation
Paulsboro Research Laboratory
Paulsboro, NJ 08066

Introduction

The performance of large fluid-bed reactors has at times differed considerably from that of smaller laboratory-scale reactors, making scale-up risky, as indicated in Figure 1. While many fluid-bed processes have been successfully scaled-up to commercial size, some notable failures have occurred, with unexpected losses in conversion efficiency and product yield. In some cases this has been related to changes in reactor hydrodynamics as size increases, with the formation of larger, faster moving gas bubbles and the development of gross circulation patterns, or "gulfstreaming." Gas tracer experiments have often been used to elucidate these phenomena and to serve as a reactor scale-up tool. Generally, the tracers used have been nonadsorbing. We used a unique tracer, SF_6, whose adsorptivity on the catalyst particles can be varied continuously over a wide range by adjusting catalyst moisture content. A series of experiments with varying adsorptivity provides more information on fluid-bed behavior than a single tracer experiment. This technique was applied in the scale-up of the methanol-to-gasoline (MTG) process.

The MTG process for converting methanol to gasoline using a zeolite catalyst, ZSM-5, was discovered by Mobil in the early 1970's. Bench-scale development was carried out in both fixed and fluid-bed reactors. The fluid-bed version was first scaled-up to a 0.1 m dia., 7.6 m tall pilot plant. Methanol feed rate to the pilot plant was typically 600 kg/day, 150 times the flow rate to the bench-scale reactor. The pilot plant has been usually referred to as a 4 Barrel per Day (B/D) pilot plant. In 1980, a five-year international project to demonstrate scale-up of the fluid-bed MTG process in a 0.6 m dia., 22 metric ton/day plant in Germany was initiated. (The demonstration plant has been referred to as the 100 B/D plant, although the design rate was 160 B/D and rates of up to 200 B/D were achieved.) The scale-up information for the demonstration plant reactor was obtained in a full-scale cold flow model (CFM) in Paulsboro, New Jersey. The tracer experiments were performed in full-scale cold flow models of the reactors to predict scale-up and to evaluate various baffle designs for improving performance. Results from gas tracer studies were incorporated in the design of the demonstration plant reactor.

Gas Tracers in Fluid-bed Scale-up

Tracer experiments have been long used to characterize chemical reactors. However, the theory developed to relate tracer response to reactor performance is strictly applicable only to homogeneous reactors. In the case of heterogeneous reactors such as fluid beds, tracer residence time distribution is only approximately related to reaction time distribution, which determines reactor performance. The tracer spends only part of its time adsorbed on the catalyst surface where chemical reactions occur.

In homogeneous systems, the response to an impulse of tracer is the residence time distribution, $f(t)$. It is defined so that the fraction of molecules that remains in the system for a time between, say t_1 and t_2, is given by the integral of $f(t)$ between these limits. If the function $r(t)$ gives the fraction of reactant

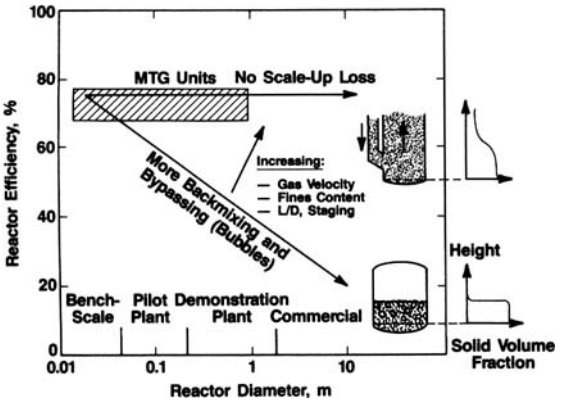

Figure 1. Potential effect of scale-up on fluid-bed reactor efficiency.

remaining unconverted after a reaction time t, under batch or plug-flow conditions, the unconverted fraction leaving the reaction system, X, is estimated by averaging this function over the residence time distribution, $f(t)$:

$$X = \int_0^\infty r(t) f(t)\, dt \tag{1}$$

Equation 1 would be exact if each element of fluid traveled through the system independently of every other element without mixing. In the special case of first-order reaction or a system of first-order reactions, where the reaction rate is a linear function of concentration, this relationship is exact regardless of the extent of mixing in the system. The unconverted fraction is then given by:

$$X = f^*(k_r) = \int_0^\infty e^{-k} r^t f(t)\, dt \tag{2}$$

where $f^*(k_r)$ is the Laplace transform of $f(t)$, evaluated at k_r, the reaction rate coefficient. This analysis requires that the reacting species all behave exactly the same as the tracer used to determine the residence time distribution. And this can usually be achieved with good precision in homogeneous reactors.

In the case of fluid-bed reactors it is more difficult to find tracers that behave identically to reactant molecules. One must consider properties such as adsorption-desorption equilibrium and rate in addition to gas-phase diffiusivity. Equation 2 will generally overpredict reactor performance even if this is done. This is true because regions of low catalyst concentration in a fluidized bed move upward faster than regions of high catalyst concentration. Thus an element of fluid with a lower than average residence time has an effective contact time that is lower still, and vice versa for elements with long residence time. This results in a contact time distribution with greater variance than the residence time distribution; hence poorer reactor efficiency would be estimated using the residence time distribution in Eq. 2.

Equation 1 or 2 can approximate conversion in a fluid bed when it approaches homogeneity. This can be the case for a bed of group A powder, with a sufficient fines fraction (at least 15% <40 μm), high gas velocity (in the turbulent fluidization regime, >0.3 m/s), and a tall bed (>4 m). Many commercial fluid-bed reactors operate in this regime. Bubble size is typically small and bubbles break up and coalesce rapidly. The two-phase appearnace of the bed gives way to a uniform, single phase. While radial density gradients were reported for group A powders (Abed, 1985), they are minimized by operating with a high fines fraction, especially in large-diameter beds. The use of horizontal baffles reduces these profiles further (Avidan et al., 1986). The homogeneous dispersion model was found to be applicable in our analysis of fluid-bed MTG scale-up under these conditions (Avidan and Edwards, 1986).

The prediction of reactor performance in the more general nonhomogeneous situations, when deviations from Eq. 2 are significant, is more difficult. In this case one generally resorts to a multizone mathematical model to match the tracer results and then predict reactor performance. The two-phase dense phase dispersion model was developed by May (1959) and by van Deemter (1961). The more general two-phase countercurrent flow model was developed by van Deemter (1967). Numerous, more complicated two-phase models that include bubble size as a parameter have also been proposed (van Swaaij, 1985). Of all two-phase model parameters, bubble size (or more correctly bubble-size distribution) has been the most troublesome to predict, especially in large-scale reactors.

Surprisingly, models containing bubble properties are used extensively in the fluidization literature. These models are seldom claimed to be more than "learning models," while actual design models in industry are simpler. In the turbulent fluidization regime voids are in a constant state of coalescence, and the bubble model has no relation to the physical picture. This is usually the case for most commercial applications of fine powders.

The countercurrent model has had more success as a design model; for example, in the development of the Shell chlorine process (van Swaaij, 1985). Model parameters need to be measured independently, or assumed. For example, minimum fluidization voidage for the dense phase is often assumed. This assumption is not very good for group A powders, especially when the fines fraction is high. Also, the two-phase physical appearance of the bed is diminished as gas velocity increases (Yerushalmi and Avidan, 1985). Nevertheless, the countercurrent model is the most appropriate representation of heterogeneous systems. We use it here in a modified form that includes adsorption effects.

Adsorbing Tracers

The results of tracer experiments in multiphase systems are quite sensitive to the extent of tracer partition between the phases. Indeed, this is the basic principle of chromatography. For fluid-bed reactors the relevant tracer property is its adsorption coefficient. Even if the bed can be approximated as homogeneous, it is necessary that the tracer have the same adsorption coefficient as the reactant for Eq. 2 to be valid. In any event, it is clear that more information about the mixing behavior of the system can be obtained by using several tracers, of different adsorption coefficients, than by using any single value.

One method of using adsorbing tracers to measure contact time distribution is described by Nauman and Buffham (1983). A pair of experiments, at two adsorption levels, gives two "washout" functions, which yield an estimate of the contact time distribution based on the simplifying assumption of proportionality between the contact time and residence time of an individual

element of tracer. This assumption cannot be true in general but may be a good approximation for certain real reactors. The two-phase dense phase dispersion model was modified to include adsorption by Bohle and van Swaaij (1978). They found that mass transfer was enhanced by adsorption in parallel with chemical reaction. The enhancement was proportional to the square root of the adsorption coefficient.

A more complex four-phase model with nonlinear dynamic adsorption/desoprtion was developed by Schlingmann et. al. (1982) to describe tracer experiments with CO_2 and argon in beds of sodium carbonate. However, we found that a two-phase model with linear equilibrium adsorption was adequate for our system. The particular model we used is the countercurrent flow model modified to include adsorption. This model is used to describe the relationship between tracer response and reactor performance. It predicts reactor efficiency at a whole range of adsorption levels, from the nonadsorption case to a highly adsorbing tracer case.

Experimental Method

Gas tracer studies were performed in full-scale cold flow models (CFM) of the 4 B/D pilot plant and the 100 B/D demonstration plant reactors. The gas tracer technique in the demonstration plant CFM is illustrated in Figure 2. Sulfur hexafluoride (SF_6) tracer was injected into the CFM reactor cone section 250 mm below the perforated plate distributor. Tracer injection was effected by switching solenoid valves. The sample probe was 1.6 mm in diameter to minimize contribution to lag time. At the probe tip, a 2 μm filter element kept the catalyst from entering the sample line. The sample probe was located 1.8 m above the catalyst bed. Experience from the pilot plant CFM had shown that a sample probe located in the catalyst bed would yield a noisy signal. The calculated theoretical and residence times were adjusted for the different average voidages in the two regions.

A commercial leak detector, with a Ni-63 source, was used to measure the response signal. The signal was proportional to the amount of tracer gas, interference from air or steam was insignificant. The signal from the detector was transmitted to a strip chart recorder (to assist the operator), and to a computer.

A typical set of runs consisted of two step-up, two step-down, and five pulse responses. Tracer data were collected at the center of the CFM, 230 mm from the center, and near the wall. At low gas velocities, <0.3 m/s, there existed a radial gradient in tracer concentration. This gradient decreased as gas velocity was increased and was negligible at the design gas velocity of 0.6 m/s. The pulse response in the center of the column was taken to represent the average response. The gas velocity was varied from 0.2 to 1.2 m/s. Only pulse responses at the design velocity are reported here.

The solids used in these experiments were typical FCC catalysts, CBZ-1 in the pilot plant CFM and CCZ-11 in the demonstration plant CFM; their properties are given in Table 1. The tracer gas adsorbed on the solids and the degree of adsorption was controlled by cofeeding steam, which also adsorbs over the solids, Figure 3. The adsorption coefficient K was defined as:

$$K = c_s/c_g \tag{3}$$

The response of the bed with and without internal baffles was

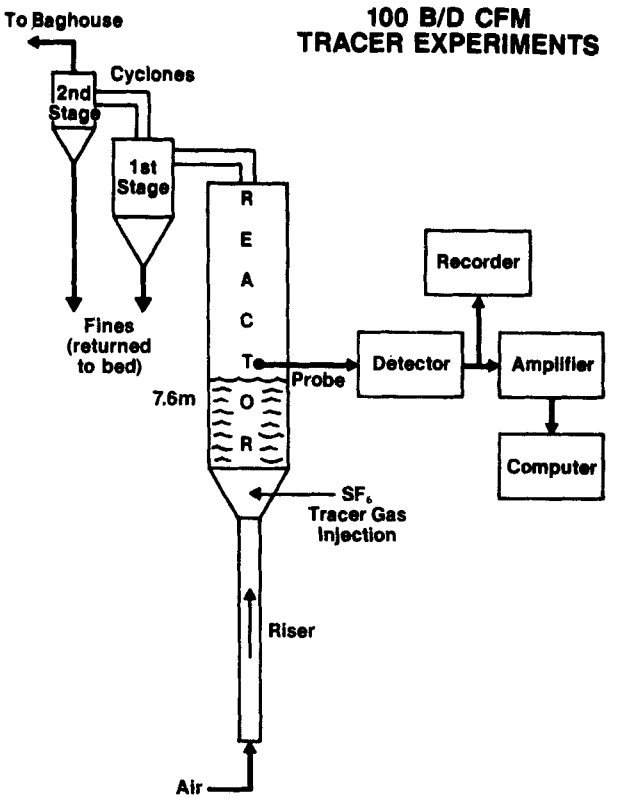

Figure 2. Gas tracer experiments in MTG demonstration plant cold flow model (CFM).

evaluated. The baffles included vertical and horizontal designs. The demonstration plant CFM baffles are illustrated schematically in Figure 4. The pilot plant CFM baffles were placed 1.3 m above the grid and the baffled section was 1.8 m long.

Typical gas tracer response curves are shown in Figure 5. These were evaluated by direct kinetic evaluation, Eq. 2, and are shown in Table 2. An alternative analysis made by first fitting the raw data with the one-dimensional axial dispersion model, as described by Avidan and Edwards (1986), yielded similar results. The tracer response curves are summarized in terms of

Table 1. Solids Properties

Particle Size Distrib. Size Range μm	Cold Flow Model (CFM) Demonstration Plant 100 B/D Catalyst CCZ-11	Pilot Plant 4 B/D Catalyst CBZ-1
0–20	0.01	0.01
20–40	0.15	0.08
40–80	0.64	0.55
80–100	0.15	0.31
>100	0.05	0.05
	Density, kg/m^3	
True	2,440	2,570
Particle	1,220	1,035
Bulk	870	640

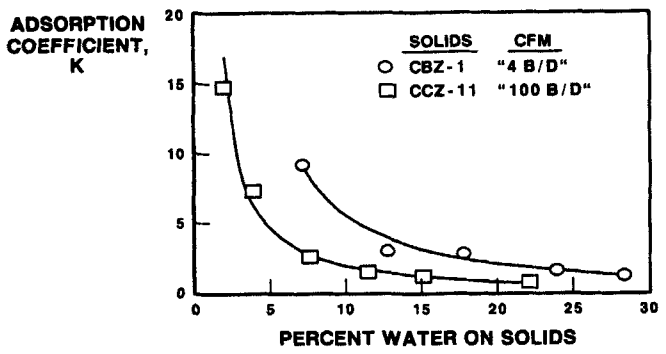

Figure 3. Effect of water on SF_6 adsorption on solids.

the following quantities: τ/τ_o is the ratio of the measured tracer residence time to that estimated for nonadsorbing gas (gas holdup/gas flow rate); σ^2/τ^2 is the dimensionless variance of the tracer response; the apparent reactor efficiency η is the ratio of the rate constant required in a plug flow reactor for a given conversion level, here 99.5%, to that required in Eq. 2 for $X = 0.005$. Apparent reactor efficiencies from the 100 B/D and 4 B/D reactors, with and without baffles, decreases as adsorption increases, Figure 6. The use of horizontal baffles increases apparent reactor efficiency in both reactors.

Operation of the demonstration plant (Gierlich et al., 1986) has confirmed the predictions of Figure 6. The scale-up from the pilot plant was successful with no loss in efficiency, and the effect of horizontal baffles was confirmed.

Countercurrent Flow Model with Adsorption

We chose the countercurrent model proposed by van Deemter (1967) to represent the results of tracer experiments. It assumes the fluidized bed to consist of two zones, an upflow zone of low solids concentration and a downflow zone of high concentration,

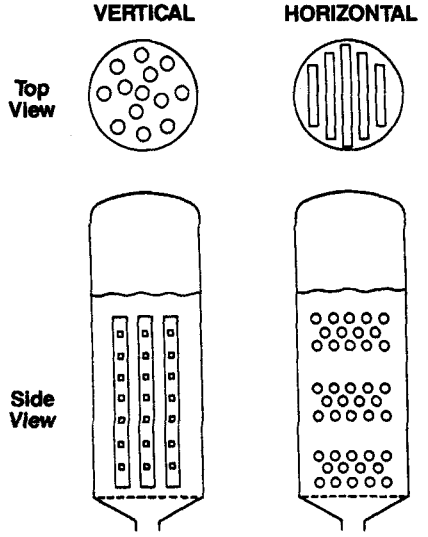

Figure 4. Demonstration plant CFM reactor internal baffles.

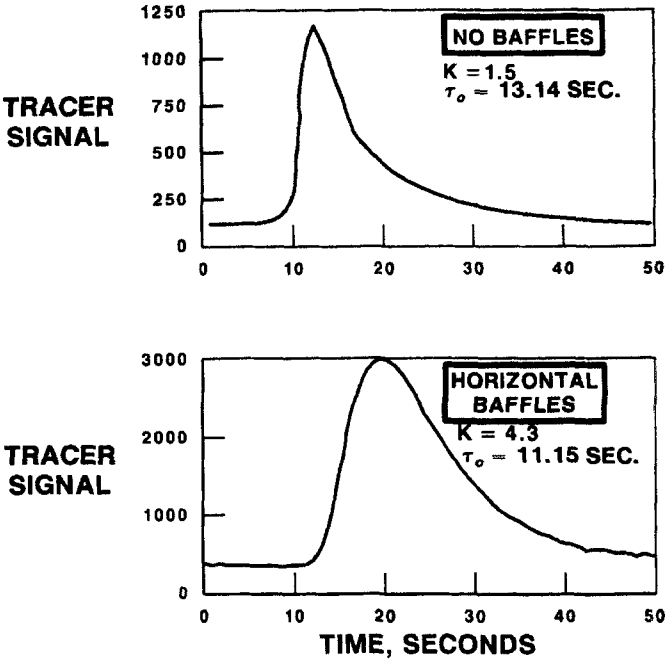

Figure 5. Examples of experimental data in demonstration plant CFM.

as shown in Figure 7. To incorporate the effects of adsorption, we assumed that tracer or reactant species were locally in adsorption equilibrium. The transient material balance equations for this model are:

$$(F + KF_s)\frac{\partial C}{\partial t} + (FV + KF_sV_s)\frac{\partial C}{\partial x} + (k + Kk_s)(C - c) + k_rF_sC = 0 \quad (4)$$

$$(f + Kf_s)\frac{\partial c}{\partial t} + (fv + Kf_sv_s)\frac{\partial c}{\partial x} + (k + Kk_s)(c - C) + k_rf_sc = 0 \quad (5)$$

Table 2. Tracer Data in Demonstration Plant CFM

Adsorption Coeff.*	τ/τ_o	σ^2/τ^2	η, Appar. Reactor Effic.** %
	No Baffles		
1.5	1.1	0.49	60
3	1.2	0.57	52
4	1.4	0.61	48
6	1.7	0.72	37
8.5	2.2	0.85	23
	Horizontal Baffles		
1.2	1.1	0.21	72
1.6	1.2	0.22	71
2.2	1.3	0.22	70
3.9	1.7	0.26	65
10.1	2.6	0.38	52

*Based on measured catalyst moisture content
**At 99.5% conversion

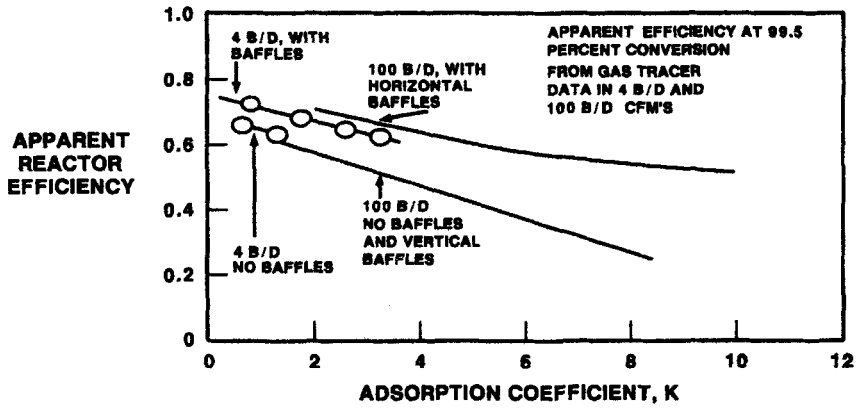

Figure 6. Effect of adsorption on measured apparent reactor efficiency.

Defining the following dimensionless groups:

$$y = x/L$$

$$\theta = \frac{tu}{L(f + Kf_s + F + KF_s)} = \frac{t}{\tau}$$

$$n = \frac{(k + k_s K)L}{u}$$

$$\beta = -\frac{(fv + Kf_s v_s)}{u}$$

$$\phi = \frac{F + KF_s}{f + Kf_s + F + KF_s}$$

$$\kappa = \frac{L(F_s + f_s)k_r}{u}$$

$$\phi_s = \frac{F_s}{f_s + F_s} \tag{6}$$

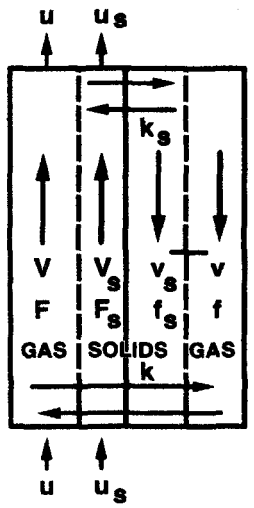

Figure 7. Countercurrent flow model (van Deemter, 1967).

these become:

$$\phi \frac{\partial C}{\partial \theta} + (1 + \beta)\frac{\partial C}{\partial y} + n(C - c) + \phi_s \kappa C = 0 \tag{7}$$

$$(1 - \phi)\frac{\partial c}{\partial \theta} - \beta \frac{\partial c}{\partial y} + n(c - C) + (1 - \phi_s)\kappa c = 0 \tag{8}$$

The tracer response of the model to an impulse input is determined by setting the chemical reaction rate term equal to zero, and imposing the appropriate initial and boundary conditions. Taking Laplace transforms yields:

$$s\phi C^* + (1 + \beta)\frac{dC^*}{dy} + n(C^* - c^*) = 0 \tag{9}$$

$$s(1 - \phi)c^* - \beta \frac{dc^*}{dy} + n(c^* - C^*) = 0 \tag{10}$$

with boundary conditions

$$y = 0: (1 + \beta)C^* - \beta c^* = 1 \tag{11}$$

$$y = 1: C^* = c^* \tag{12}$$

The Laplace transform of tracer impulse response is then:

$$f^*(s) = c^*(s)|_{y=1} \tag{13}$$

The performance of the model as a reactor is found by setting the time derivatives in Eqs. 7 and 8 to zero, and setting boundary conditions. This gives:

$$\kappa\phi_s C + (1 + \beta)\frac{dC}{dy} + n(C - c) = 0 \tag{14}$$

$$\kappa(1 - \phi_s)c - \beta \frac{dc}{dy} + n(c - C) = 0 \tag{15}$$

with boundary conditions:

$$y = 0: (1 + \beta)C - \beta c \tag{16}$$

$$y = 1: C = c \tag{17}$$

The amount of unconverted reactant is the.

$$X = c|_{y=1} \tag{18}$$

Comparing Eqs. 9–13 with Eqs. 14–18, we see that the Laplace transform of the tracer response to a unit impulse $f^*(s)$ is exactly the same function as the fraction of unconverted reactant, $X(\kappa)$, provided $\phi = \phi_s$. The implication of this is that when $\phi = \phi_s$ the reactor performance for a first-order reaction can be calculated from Eq. 2; just as for homogeneous reaction systems. It can be seen from Eq. 6 that there are two general conditions where $\phi = \phi_s$. One is when $f_s/f = F_s/F$, or, in other words, when the solids concentration is uniform everywhere so that the system is in fact homogeneous. The other is when $K \to \infty$. In this case the tracer spends almost all its time in the system in contact with the solid catalyst, so that the tracer residence time distribution is again the same as the reaction time distribution.

The solution to Eqs. 9–13 or 14–18, following van Deemter (1967), is given in the Appendix, along with a formula for the variance of the residence time distribution (which had an error in the original reference).

Behavior of Model and Significance

Some examples of model predictions are shown in Figures 8 and 9. The ordinate of these graphs is reactor efficiency at 99.5% conversion compared to an ideal plug flow reactor. Both the true reactor efficiency (broken lines), calculated from the solution to Eqs. 14–18, and the apparent reactor efficiency (solid lines), from Eq. 1 and the solution to Eqs. 9–13, are shown. The parameters were chosen by assuming that the gas and solids velocity are equal to each other in each zone. Choosing values for the overall void fraction of the bed, ϵ_o, and the void fraction in each zone, ϵ_u and ϵ_d, then determines the parameters F, F_s, f, f_s, v, and V as follows:

$$F = [(1 - \epsilon_u)\, p + \epsilon_u] \frac{\epsilon_o - \epsilon_d}{\epsilon_u - \epsilon_d}$$

$$F_s = (1 - \epsilon_u)\,(1 - p) \frac{\epsilon_o - \epsilon_d}{\epsilon_u - \epsilon_d}$$

$$f = [(1 - \epsilon_d)\, p + \epsilon_d] \frac{\epsilon_u - \epsilon_o}{\epsilon_u - \epsilon_d}$$

$$f_s = (1 - \epsilon_d)\,(1 - p) \frac{\epsilon_u - \epsilon_o}{\epsilon_u - \epsilon_d}$$

$$v = v_s = \frac{F_s u}{fF_s - f_s F}$$

$$V = V_s = -\frac{f_s v}{F_s} \tag{19}$$

These equations are based on the material balance defined in Figure 7. Note that in this model the particle pore volume is included in the gas volume. We also assume that the transfer

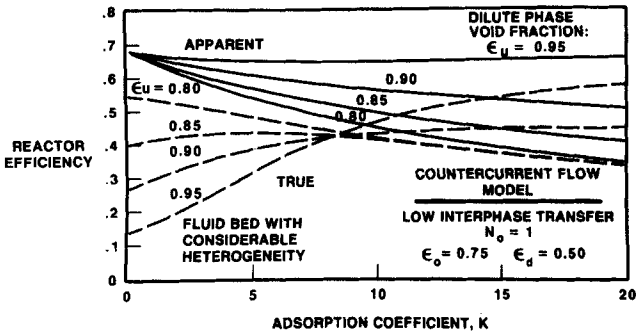

Figure 8. Effect of adsorption on reactor efficiency for a fluid bed with considerable heterogeneity.

coefficients k and k_s are equal. Thus the only remaining parameters are $n_o = kL/u$ and the adsorption coefficient K.

Figure 8 shows the effect of the dilute zone void fraction ϵ_u when interphase transfer is low, $n_o = 1$. High values of ϵ_u give low values of true reactor efficiency because the gas flowing in the dilute phase contacts very little catalyst. As the reactant adsorption coefficient increases, this situation initially improves because of the increasing mass transfer parameter $n_o(1 + K)$. As K increases further, however, the backflow effect eventually brings the efficiency down again as the system approaches complete mixing. In contrast, the apparent efficiency based on tracer response is almost completely insensitive to this parameter when the tracer is nonadsorbing (all apparent curves in Figure 8 meet at an efficiency of 67% for $K = 0$). Only when the tracer adsorption coefficient is large does the tracer response begin to give a true picture of reactor behavior, assuming of course that the reacting species is also strongly adsorbing. Note however that the shape of the curves of apparent efficiency vs. K for high values of ϵ_u are much different from the actual data shown in Figure 6. Thus the availability of tracer results over a wide range of adsorptivity provides a much better basis for discriminating models than would nonadsorbing tracer data alone.

Figure 9 shows similar calculations using parameter values that more closely match the results in Figure 6. Here the dilute phase void fraction (0.77) has been taken to be very close to the overall void fraction (0.75). This results in a much more homogeneous system that corresponds with the actual appearance of the bed. In this case the apparent efficiency actually gives a good estimate of the true efficiency from the two-phase model.

Conclusions

The major results and conclusions from our work are:

1. A series of gas tracer experiments with varying levels of tracer adsorption coefficients is much more effective for model discrimination, and hence for reactor performance prediction, than a single level of tracer adsorption. The use of SF_6 tracer with varying catalyst moisture levels is an effective means of doing this.

2. Under properly chosen conditions a turbulent fluidized bed approaches homogeneity so that the apparent reactor efficiency from tracer experiments is a good approximation to actual reactor efficiency. It is important, however, that the tracer used have the same adsorption behavior as the reactant.

3. Horizontal baffles are particularly effective in improving fluid-bed reactor performance.

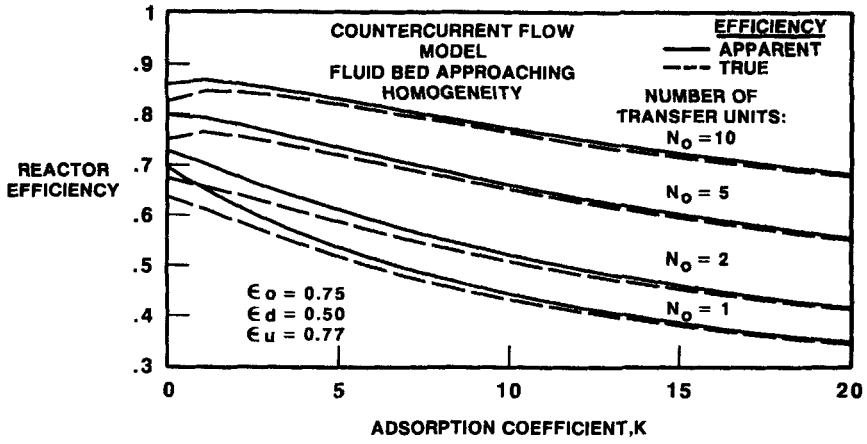

Figure 9. Effect of adsorption on reactor efficiency for a fluid bed approaching homogeneity.

Acknowledgment

The 100 B/D Project was a joint effort by Union Rheinische Braunkohlen Kraftstoff AG, Uhde GmbH, and Mobil Research and Development Corporation, supported in part by the U.S. Department of Energy and the Federal Republic of Germany Bundesministerium fuer Forschung und Technologie.

Notation

c = concentration in downflow phase gas
C = concentration in upflow phase gas
c_g = tracer concentration in gas phase, including solids pores
c_s = tracer concentration in solid phase, excluding pores
f = volume fraction, downflow phase gas
f_s = volume fraction, downflow phase solids
$f(t)$ = residence time distribution
F = volume fraction, upflow phase gas
F_s = volume fraction, upflow phase solids
k = gas transfer coefficient
K = adsorption coefficient
k_r = reaction rate coefficient
k_s = solids transfer coefficient
L = bed height
n_o = number of mass transfer units
p = catalyst porosity
$r(t)$ = fraction of reactant remaining unconverted after a reaction time t
t = time
u = superficial gas velocity
u_s = superficial solids velocity
v = linear velocity of downflow phase gas
V = linear velocity of upflow phase gas
v_s = linear velocity of downflow phase solids
V_s = linear velocity of upflow phase solids
x = axial coordinate
X = unconverted reactant fraction

Greek Letters

ϵ_o = overall bed void fraction
ϵ_d = downflow phase void fraction
ϵ_u = upflow phase void fraction
σ^2 = variance of tracer residence time distribution
τ = mean residence time of tracer = $L[F + f + K(F_s + f_s)]/u$
τ_o = mean residence time of nonadsorbing tracer = $L(F + f)/u$
η = reactor efficiency, ratio of rate coefficient required in plug flow to that required in actual reactor for a given conversion

Appendix

The solution to Eqs. 9–13 is, following van Deemter (1967):

$$C^* = \frac{\lambda_2 - \lambda_1}{(\lambda_2 + s)\, e^{-\lambda_1} - (\lambda_1 + s)\, e^{-\lambda_2}} \tag{A1}$$

where

$$\lambda^2 - \frac{n + (1 + \beta)(1 - \phi)\, s - \beta\phi s}{\beta(1 + \beta)}\lambda - \frac{ns + \phi(1 - \phi)s^2}{\beta(1 + \beta)} = 0 \tag{A2}$$

The solution to Eqs. 14–18 is:

$$C = \frac{\lambda_2 - \lambda_1}{(\lambda_2 + \kappa)\, e^{-\lambda_1} - (\lambda_1 + \kappa)\, e^{-\lambda_2}} \tag{A3}$$

where

$$\lambda^2 - \frac{n + (1 + \beta)(1 - \phi_s)\,\kappa - \beta\phi_s\kappa}{\beta(1 + \beta)} \cdot \lambda - \frac{n\kappa + \phi_s(1 - \phi_s)\,\kappa^2}{\beta(1 + \beta)} = 0 \tag{A4}$$

The variance of the tracer response, from Eqs. A1 and A2, is

$$\sigma^2 = \frac{2}{n}(1 - \phi + \beta)^2 \cdot \left\{1 - \frac{\beta(1 + \beta)}{n}\left[1 - \exp\left(-\frac{n}{\beta(1 + \beta)}\right)\right]\right\} \tag{A5}$$

Literature Cited

Abed, R., "Characterization of Hydrodynamic Nonuniformity in Large Fluidized Beds," *Ind. Eng. Chem. Fundam.*, **24**, 78 (1985).

Avidan, A. A., and M. Edwards, "Modeling and scaleup of Mobil's Fluid-Bed MTG Process," *Fluidization*, V. K. Ostergaard, ed., Engineering Foundation, New York (1986).

Avidan, A. A., R. M. Gould, and A. Y. Kam, "Operation of a Circulat-

ing Fluid-Bed Cold Flow Model of the 100 B/D MTG Demonstration Plant," *Circulating Fluidized Bed Technology*, P. Basu, ed., Pergamon, Toronto (1986).
Bohle, W., and W. P. M. van Swaaij, "The Influence of Gas Adsorption on Mass Transfer and Gas Mixing in a Fluidized Bed," *Fluidization*, J. F. Davidson and D. L. Keairns, eds., Cambridge, London, 167 (1978).
Gierlich, H.-H., W. Dolkemeyer, A. A. Avidan, and N. Thiagarajan, "Umwandlung von Methanol Zu Benzin nach dem Wirbelbett-Verfahren," *Chem.-Ing.-Tech.*, **58**,(3), 238 (1986).
Nauman, E. B., and B. A. Buffham, *Mixing in Continuous Flow Systems*, Wiley, New York (1983).
May, W. G., "Fluidized-Bed Reactor Studies," *Chem. Eng. Prog.*, **55**,(12), 49 (1959).
Schlingmann, H., M. Thoma, D. Wippern, H. Helmrich, and K. Schuegerl, "Influence of Bed Structure and Tracer Sorption on the RTD in Fluidized-Bed Reactors," *Residence Time Distribution Theory in Chemical Engineering*, A. Pethoe, R. D. Noble, eds., Verlag Chemie GMbH, Weinheim, 181 (1982).
van Deemter, J. J., "Mixing and Contacting in Gas-Solid Fluidized Beds," *Chem. Eng. Sci.*, **13**, 143 (1961).
———, "The Counter-Current Flow Model of a Gas-Solids Fluidized Bed," *Proc. Int. Symp. Fluidization*, A. H. H. Drinkenburg, ed., Netherlands Univ. Press, Amsterdam, 334 (1967).
van Swaaij, W. P. M., "Chemical Reactors," *Fluidization*, 2nd ed., J. F. Davidson, R. Clift, D. Harrison, eds., Academic Press, London, 595 (1985).
Yerushalmi, J., and A. A. Avidan, "High-Velocity Fluidization," *Fluidization*, 2nd ed., J. F. Davidson, R. Clift, D. Harrison, eds., Academic Press, London, 225 (1985).

Manuscript received Dec. 16, 1986, and revision received Feb. 27, 1987.

Errata

In the article entitled "Study of Coal Gasification in an Experimental Fluidized Bed Reactor" by D. Neogi, C. C. Chang, W. P. Walawender, and L. T. Fan (**32**, p. 17, Jan., 1986), Eq. 14 should read:

$$R_{1e} = S(k_1 C_{4e} + 2k_2 C_{2e}) - R_{sr} - C_g C_1 \qquad (14)$$

In this equation, a typographical error was made which has no effect on the numerical results.

In the article entitled "Simulation of Desulfurization in a Fluidized-Bed Limestone Reactor" by Tho-Ching Ho, Hom-Ti Lee, and J. R. Hopper (**32**, p. 1754, Oct., 1986), the exponent of ρ_p in Eq. 6 should be 0.376 instead of 0.736. We acknowledge Dr. S. Prasad of the Regional Research Laboratory of Jorhat, India for bringing the error to our attention.